

4

David Taylor Research Center

Bethesda, MD 20884-5000

AD-A207 595

DTRC-89/005 April 1989

Ship Hydromechanics Department
Research and Development Report

A Lifting-Surface Program for Contrarotating Propellers


by

Benjamin Y.-H. Chen
Arthur M. Reed

Presented at the Symposium on Hydrodynamic Performance
Enhancement for Marine Applications
Newport, Rhode Island, 31 October - 1 November 1988

DTRC-89/005 A Lifting-Surface Program for Contrarotating Propellers

**BEST
AVAILABLE COPY**

 **DTIC**
ELECTE
MAY 11 1989
S H D



Approved for public release; distribution is unlimited.

89 5 11 126

MAJOR DTRC TECHNICAL COMPONENTS

- CODE 011 DIRECTOR OF TECHNOLOGY, PLANS AND ASSESSMENT
 - 12 SHIP SYSTEMS INTEGRATION DEPARTMENT
 - 14 SHIP ELECTROMAGNETIC SIGNATURES DEPARTMENT
 - 15 SHIP HYDROMECHANICS DEPARTMENT
 - 16 AVIATION DEPARTMENT
 - 17 SHIP STRUCTURES AND PROTECTION DEPARTMENT
 - 18 COMPUTATION, MATHEMATICS & LOGISTICS DEPARTMENT
 - 19 SHIP ACOUSTICS DEPARTMENT
 - 27 PROPULSION AND AUXILIARY SYSTEMS DEPARTMENT
 - 28 SHIP MATERIALS ENGINEERING DEPARTMENT

DTRC ISSUES THREE TYPES OF REPORTS:

1. **DTRC reports, a formal series**, contain information of permanent technical value. They carry a consecutive numerical identification regardless of their classification or the originating department.
2. **Departmental reports, a semiformal series**, contain information of a preliminary, temporary, or proprietary nature or of limited interest or significance. They carry a departmental alphanumeric identification.
3. **Technical memoranda, an informal series**, contain technical documentation of limited use and interest. They are primarily working papers intended for internal use. They carry an identifying number which indicates their type and the numerical code of the originating department. Any distribution outside DTRC must be approved by the head of the originating department on a case-by-case basis.

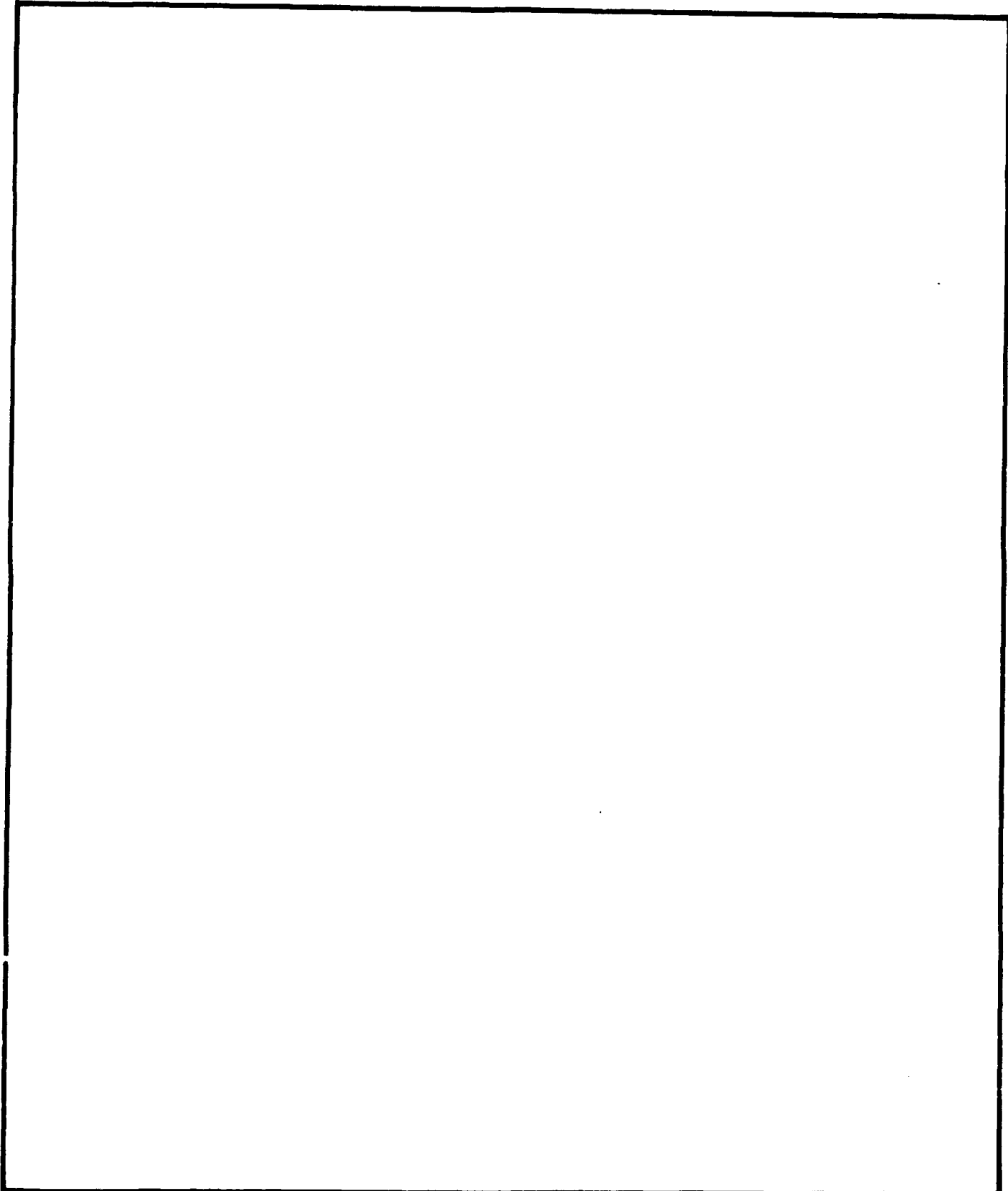
UNCLASSIFIED

SECURITY CLASSIFICATION OF THIS PAGE

REPORT DOCUMENTATION PAGE				Form Approved OMB No 0704-0188	
1a REPORT SECURITY CLASSIFICATION UNCLASSIFIED			1b RESTRICTIVE MARKINGS		
2a SECURITY CLASSIFICATION AUTHORITY		3 DISTRIBUTION AVAILABILITY OF REPORT APPROVED FOR PUBLIC RELEASE; DISTRIBUTION IS UNLIMITED.			
2b DECLASSIFICATION/DOWNGRADING SCHEDULE		5 MONITORING ORGANIZATION REPORT NUMBER(S)			
4 PERFORMING ORGANIZATION REPORT NUMBER(S) DTRC-89/005			7a NAME OF MONITORING ORGANIZATION		
6a NAME OF PERFORMING ORGANIZATION David Taylor Research Center	6b OFFICE SYMBOL (If applicable) Code 1544	7b ADDRESS (City, State, and ZIP Code)			
6c ADDRESS (City, State, and ZIP Code) Bethesda, MD 20084-5000		9 PROCUREMENT INSTRUMENT IDENTIFICATION NUMBER			
8a NAME OF FUNDING SPONSORING ORGANIZATION Office of Naval Technology	8b OFFICE SYMBOL (If applicable) Code 21	10 SOURCE OF FUNDING NUMBERS			
8c ADDRESS (City, State, and ZIP Code) 800 N. Quincy St. Arlington, VA 22217		PROGRAM ELEMENT NO 63543N	PROJECT NO 4B101AH	TASK NO Sf-43-434U	WORK UNIT ACCESSION NO
11 TITLE (Include Security Classification) A LIFTING-SURFACE PROGRAM FOR CONTRAROTATING PROPELLERS					
12 PERSONAL AUTHOR(S) Chen, Benjamin Y.-H. and Reed, Arthur M.					
13a TYPE OF REPORT Final	13b TIME COVERED FROM _____ TO _____	14 DATE OF REPORT (Year, Month, Day) 1989 April	15 PAGE COUNT 20		
16 SUPPLEMENTARY NOTATION Presented at the Symposium on Hydrodynamic Performance Enhancement for Marine Applications, Newport, Rhode Island, 31 October--1 November 1988					
17 COSATI CODES			18 SUBJECT TERMS (Continue on reverse if necessary and identify by block number)		
FIELD	GROUP	SUB-GROUP	Contrarotating Propellers Lifting-Surface Program		
19 ABSTRACT (Continue on reverse if necessary and identify by block number)					
<p>A new lifting-surface computer program for a set of CR propellers has been developed based on a modified version of the MIT lifting-surface design program with hub effects. This program automatically computes the velocities induced by one propeller on the other. In addition, the hub portion of the program is modified to account for the velocities induced by one propeller on the hub of the opposite propeller. The data from LDV measurements of induced velocities are used to adjust the shape and distribution of the wakes shed from the two propellers. A comparison between the conventional and the new methods for the design of a set contrarotating propellers for a surface ship is also given.</p>					
20 DISTRIBUTION AVAILABILITY OF ABSTRACT <input checked="" type="checkbox"/> UNCLASSIFIED AND LIMITATION <input type="checkbox"/> SAME AS RPT <input type="checkbox"/> DTRC USERS			21 ABSTRACT SECURITY CLASSIFICATION UNCLASSIFIED		
22a NAME OF RESPONSIBLE INDIVIDUAL Benjamin Y.-H. Chen			22b TELEPHONE (Include Area Code) (202) 227-1450	22c DTRC NUMBER Code 1544	

UNCLASSIFIED

SECURITY CLASSIFICATION OF THIS PAGE



CONTENTS

	Page
ABSTRACT	1
INTRODUCTION	1
METHODOLOGY.	2
TRADITIONAL DESIGN PROCEDURE.	2
NEW DESIGN PROCEDURE.	3
SLIPSTREAM CONTRACTION.	4
SAMPLE CALCULATION FOR A CR PROPELLER DESIGN	4
SUMMARY.	12
CONCLUSIONS AND RECOMMENDATIONS.	12
ACKNOWLEDGMENTS.	12
REFERENCES	12

FIGURES

1. A CR propeller set.	1
2. Velocity diagram of a CR propeller set.	2
3. Flow chart of CR lifting-line program	3
4. Flow chart of conventional CR lifting-surface program	3
5. Flow chart of new CR lifting-surface program.	4
6. Slipstream contraction of a CR propeller using LDV measurements	5
7. Comparison of radial distribution of axial velocity induced by AFT propeller on forward propeller	5
8. Comparison of radial distribution of radial velocity induced by AFT propeller on forward propeller.	6
9. Comparison of radial distribution of tangential velocity induced by AFT propeller on forward propeller	6
10. Comparison of radial distribution of pitch/diameter ratio for forward propeller	7

<input checked="" type="checkbox"/>
<input type="checkbox"/>
<input type="checkbox"/>



Dist	Codes
	Mail and/or
	Special
A-1	

FIGURES (Continued)

	Page
11. Comparison for radial distribution of camber ratio for forward propeller	8
12. Comparison of open water efficiency, thrust coefficient, and torque coefficient vs. drag coefficient for forward propeller.	8
13. Comparison of radial distribution of axial velocity induced by forward propeller on AFT propeller	9
14. Comparison of radial distribution of radial velocity induced by forward propeller on AFT propeller	9
15. Comparison of radial distribution of tangential velocity induced by forward propeller on AFT propeller	10
16. Comparison of radial distribution of pitch/diameter ratio for AFT propeller	10
17. Comparison of radial distribution of camber ratio for AFT propeller	11
18. Comparison of open water efficiency, thrust coefficient, and torque coefficient vs. drag coefficient for AFT propeller	11

A LIFTING-SURFACE PROGRAM OF CONTRAROTATING PROPELLERS

Benjamin Y.-H. Chen and Arthur M. Reed
David Taylor Research Center
Bethesda, Maryland 20084-5000

ABSTRACT

A new lifting-surface computer program for a set of CR propellers has been developed based on a modified version of the MIT lifting-surface design program with hub effects. This program automatically computes the velocities induced by one propeller on the other. In addition, the hub portion of the program is modified to account for the velocities induced by one propeller on the hub of the opposite propeller. Data from LDV measurements of induced velocities have been used to adjust the shape and distribution of the wakes shed from the two propellers. A comparison between the conventional and the new methods for the design of a set contrarotating propellers for a surface ship is also given.

I. INTRODUCTION

Over the past several years, the application of contrarotating (CR) propellers on surface ships has been reemphasized because of interest in utilizing lighter and more efficient electrical propulsion systems. This interest has been heightened by the potential of CR propellers to achieve increased propulsive efficiency and increased cavitation inception speeds. A CR propeller set is shown in Fig. 1.

Four decades ago most research on CR propellers was experimental, and design techniques were empirical. Since that time, analysis techniques have developed so that today there are a number of sophisticated lifting-line and lifting-surface techniques available for use in design. One of the earliest design techniques for CR propellers was developed by Lerbs (2). Lerb's method was further refined into a usable design technique by Morgan (3). Both Lerbs and Morgan relied on classical circulation theory (4,5) for single propellers as the basis of their methods. To determine the forces and induced flow field, they applied lifting-line theory for

moderately loaded, wake adapted single propellers to the forward and aft propellers individually so that the force and induced flow field could be determined. The variations of inflow velocity (time-average) in the axial and tangential directions and the streamline contraction in the slipstream of the forward propeller were treated approximately to account for the mutual interactions between the two propellers.

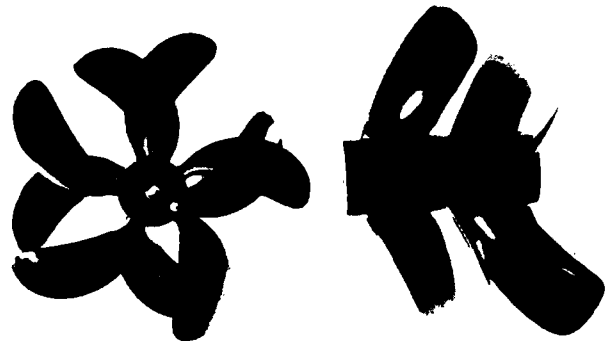


FIG. 1. A CR PROPELLER SET

Following Morgan's work, two computer programs were developed. Caster and LaFone (6) developed a CR lifting-line program based on the lifting-line program for single screw propellers. This program incorporated field point velocity computations to determine the interaction velocities between the two proximate propellers in an iterative procedure. Nelson (7) developed lifting-line as well as lifting-surface programs. He showed a successful design for CR propellers on torpedoes using the circulation distribution with finite values at the root. Both Caster's and Nelson's lifting line programs use the same approach, but differ somewhat in the options that are available to the user and the techniques by which the details are carried out.

Cox (8) chose the Caster and LaFone computer code as the basis of his method, but with several revisions as follows: 1 - Cox used the induced axial

All notations in this report are in accordance with the International Towing Tank Conference (ITTC) Standard Symbols (1).

velocities in the propeller planes to determine the mass flow rate for each propeller, and allowed that the diameter of the downstream propeller to be specified directly, regardless of the mass flow rate. Caster's program used an approximation due to Lerbs to determine the appropriate diameter for the aft propeller; 2 - Both programs use FPV-7 to calculate the velocities induced by one propeller on the other. However, Cox treated these velocities at radii smaller than the diameter of the forward propeller hub. Thus his program could readily deal with tapered hubs, which Caster's program could not.

Another, more recent, lifting-line computer program for the design of CR propellers was developed by Reed (9). It was also based on the Caster and Lafone method, and it incorporated many of the improvements due to Cox. In addition, the program incorporated improved methods for computing the velocities induced by one propeller on the other. These new methods have decreased the time required for the induced velocity calculations by more than 90 percent, substantially reducing the time required for the total lifting-line design.

In the preliminary design stage, lifting-line theory is a very useful tool. The dependence of forces and efficiency on such parameters as angular velocity diameter, blade outline, blade numbers, and circulation distribution can be determined economically through parametric calculations. Since CR propeller design involves a large number of design parameters and the calculation of mutual interactions between two propellers, an economical lifting-line tool is particularly important for CR propeller design. Lifting-line theory alone, however, can neither determine the final meanline distribution and radial pitch variation accurately nor can it predict interactions between two adjacent propellers satisfactorily. For the final design stage, lifting-surface theory must be employed in order to incorporate three-dimensional flow field effects. The traditional design procedure, described in detail in section II, employs a single propeller lifting-surface program to determine blade final pitch and camber for each blade row separately. In this traditional procedure, the interaction velocities between the propellers are those from the lifting-line model, not the lifting-surface model. Also, this procedure will not allow zero net circulation at the hub for the two propellers.

More recently, a customized lifting-surface computer program for the detailed design of the individual propellers of a CR set has been developed to strengthen the traditional design procedure. This design tool automatically computes the velocities induced by one propeller on the other. Additionally, it accounts for the hub of each propeller in the design of the set (a factor which is of greater importance for CR propellers than for single rotation propellers), and allows finite circulation at the hub of each propeller (the net circulation for the two propellers at the hub should be zero). The shape and distribution of the wakes shed from the two propellers, which is particularly important for the aft propeller, is adjusted using data from Laser Doppler Velocimetry (LDV) measurements of induced velocities around a pair of CR propellers. A sample calculation shows the comparisons between the conventional and the new method on a CR propeller design for a surface ship.

II. METHODOLOGY

As stated before, one of the major tasks in CR propeller design is to obtain the induced velocities,

which include the self-induced velocity and the induced velocity from the other blade row. Fig. 2 shows the velocity diagram for a CR propeller set. The details of the traditional design procedure and the new design procedure will be described in this section.

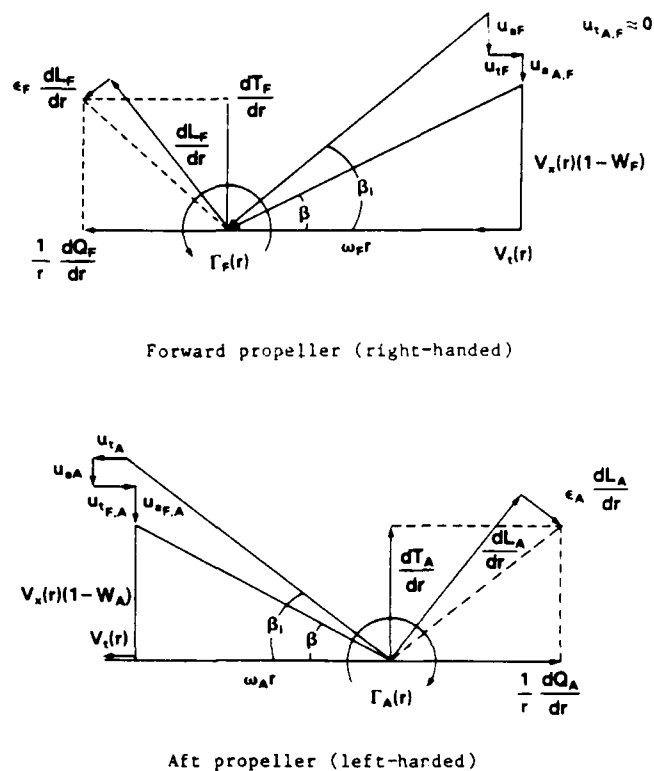


FIG. 2 VELOCITY DIAGRAM OF A CR PROPELLER SET

1. Traditional Design Procedure

A flow chart for the traditional design procedure for a CR propeller set is shown in Figs. 3 and 4. In Fig. 3, the lifting-line program is used to design the forward propeller using the inflow from wake measurements. Without considering the effect of the aft propeller, the results of the lifting-line program are the characteristics of the forward propeller. Meanwhile, the field point velocities induced by the forward propeller on the aft propeller are computed by the internal field point velocity program. The diameter of the aft propeller is determined based on mass flow conservation, and the characteristics of the aft propeller are obtained through lifting-line calculations using the combination of the induced velocities from the forward propeller and the wake measured at the aft propeller position. Once the aft propeller lifting-line calculation is complete, the field point velocities induced by the aft propeller on the forward propeller are computed and incorporated into the wake for the forward propeller. The lifting-line design is iterated through the above procedure a second time to account for the interaction effects between both propellers.

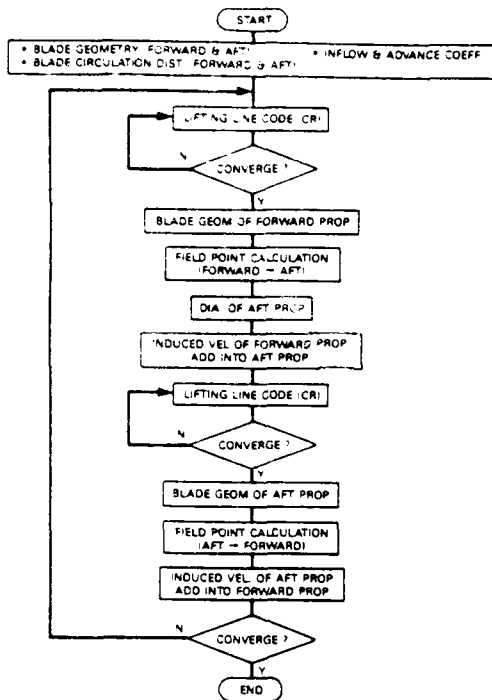


FIG. 3 FLOW CHART OF CR LIFTING-LINE PROGRAM

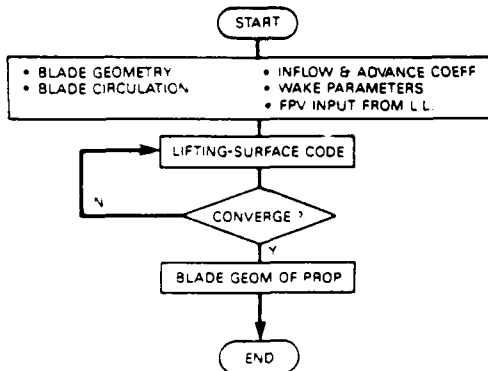


FIG. 4 FLOW CHART OF CONVENTIONAL CR LIFTING-SURFACE PROGRAM

As shown in Fig. 4, the results of the lifting-line calculations provide information (principally circulation, hydrodynamic pitch distribution, and induced velocities between blade rows) to the single propeller lifting-surface program which determines the final blade pitch and camber. Two questions are raised by using the above design procedure. First, the onset flows of the lifting-surface procedures are covered over from the lifting-line procedure. In other words, the field point velocities induced by one propeller on the other are based on the preliminary blade characteristics through lifting-line design. Second, the slipstream contraction of a CR set should be different from that of a single propeller. To improve upon the above procedure, a new design methodology, described in this report, has been developed.

2. New Design Procedure

The CR lifting-surface program is based on the MIT lifting-surface computer program, PBD-11 (10) which includes hub image effects. PBD-11 determines the propeller blade shape for a prescribed circulation distribution and a given hub geometry. The vortex lattice approach is used to represent the blades and their wakes. The hub is represented by a distribution of vortices which ends at the hub apex. By taking account of the hub effect, PBD-11 allows non-zero circulation at the hub of a propeller, a factor which seems to be more significant for CR propellers than for single rotation propellers. Additionally, its wake model is more realistic.

A vortex/source lattice method has been employed in the present field point velocity computation scheme (Kerwin (11)). The discretized version of a propeller is comprised of a blade, its wake and the hub. Following Greeley and Kerwin (12), the wake is composed of a transition wake and an ultimate wake. The vortex sheet tends to contract and roll up in the transition wake. A single helical tip vortex and a hub vortex forms the ultimate wake.

The details of the vortex/source lattice method are described as follows. The line source strength, q_{nm} due to thin wing theory and the spanwise vortex strengths, $\Gamma_{nm}(s)$, due to the normal boundary condition constitute the primary singularities. The first index, n , stands for chordwise position and the second index, m , spanwise position. Based on the conservation of vorticity, the secondary singularities include the chordwise vortices, $\Gamma_{nm}(c)$, the transition wake trailing vortices, $\Gamma_{nm}(tw)$, the ultimate tip vortex, $\Gamma_n(t)$, and the hub vortex, $\Gamma_j(h)$, where j is the j th panel. A special treatment, shown in Greeley and Kerwin (12) and in Kerwin and Lee (13), is required for the chordwise vortices originating from the outer end of the tip panel.

Induced velocities due to the blade, its vortex wake and the hub can be found by summing the product of the singularity strengths with the corresponding velocity influence functions, \vec{H}_{nm}^r and \vec{H}_{nm}^q . Velocity influence functions are defined as vector velocities which a line vortex and source of unit strength induce at the field point. These influence function velocities are computed for lattice elements with the indices n and m .

According to Kerwin (11), the induced velocity due to the spanwise vortices and sources is

$$\vec{V}_s = \sum_{n=1}^N \sum_{m=1}^M \Gamma_{nm}(s) \vec{H}_{nm}^r \quad (1)$$

and

$$\vec{V}_q = \sum_{n=1}^N \sum_{m=1}^M q_{nm} \vec{H}_{nm}^q, \quad (2)$$

where N and M are the number of panels over the chord and span, respectively.

The induced velocity due to the chordwise vortices and the separated sheet at the tip is

$$\vec{V}_c = \sum_{n=1}^{N-1} \sum_{m=1}^M \Gamma_{nm}(c) \vec{H}_{nm}^r + \sum_{n=1}^N \sum_{l=1}^{N-n+1} \Gamma_{nl}(ct) \vec{H}_{nl}^r, \quad (3)$$

where the symbol l in the second summation represents the individual chordwise vortex elements due to the outer end of the n 'th spanwise vortex.

The induced velocity due to the transition wake is

$$\vec{V}_{tw} = \sum_{m=1}^{M+1} \sum_{n=1}^{N_w(m)-1} \Gamma_{nm} (tw) \vec{H}_{nm} \Gamma, \quad (4)$$

where $N_w(m)$ stands for the number of points describing the path of the trailing vortex shed from the inner end of $\Gamma_{Nm}^{(s)}$. The inner radius of the transition wake should be exactly the same as the hub geometry. The collection point of the separated tip vortex contributes the $(M+1)$ st transition wake element.

The induced velocity due to the ultimate tip vortex is

$$\vec{V}_t = \sum_{n=1}^{Nu-1} \Gamma_n^t \vec{H}_n \Gamma, \quad (5)$$

where Nu represents the number of points which form the piecewise linear approximation to the helical ultimate wake. The first point of the helical ultimate wake agrees with the last point in the tip element of the transition wake.

Finally, according to Wang (10), the induced velocity due to the hub vortex is

$$\vec{V}_h = \sum_{i=1}^{NT} \sum_{j=1}^{NT} \Gamma_j (h) \vec{H}_{ij} \Gamma, \quad (6)$$

where \vec{H}_{ij} is the velocity induced at the i 'th control point by the j 'th panel. $NT = NR * NH$ is the total number of panels. Each panel consists of two helical vortex elements and two vortex ring elements. NH is the number of helical vortices on the hub between two blades. $NR = N_{N1} + N_N + N_{N2}$ is the number of vortex rings, where N_{N1} is the number of vortex rings between the blade leading edge and the blade trailing edge, and N_{N2} is the number of vortex rings between the blade trailing edge and the hub apex. The total induced velocity due to blade and wake and hub vortices is

$$\vec{V} = \vec{V}_s + \vec{V}_q + \vec{V}_c + \vec{V}_{tw} + \vec{V}_t + \vec{V}_h. \quad (7)$$

A flow chart for the new CR lifting-surface program is shown in Fig. 5. The input includes the blade characteristics (such as blade and hub geometry, and circulation from the results of lifting-line calculations), inflow information, wake parameters, and locations at which field point velocities induced by one propeller are obtained, the field point velocities on the other propeller are automatically calculated. These field point velocities, which result from two sources (one from blade and wake vortices and the other from the hub vortex), will be treated as additional onset flows when the other propeller is achieved, the program will automatically compute the field point velocities induced on the first propeller. The first propeller will be redesigned using the new onset flow. This iterative procedure is followed until the field point velocities induced by one propeller on the other show no significant change.

3. Slipstream Contraction

As flow passes through a propeller, the streamlines must contract because the propeller imparts an axial acceleration to the flow passing through the propeller. The contraction of the slipstream is a

well known phenomenon from the evidence of theoretical analysis as well as experimental measurements. It is very difficult to accurately predict the trajectory of single streamlines analytically due to the effects of nonlinear and three-dimensional characteristics of the flow. This is especially because the vortex sheets tend to roll up in the slipstream. Up to this point, the streamline contraction of a CR set has seldomly been included in the design or analysis of CR propellers. Nagle and McMahon (14) measured the flow velocity in the vicinity of a set of CR research propellers (propellers 4866 and 4867) using Laser Doppler Velocimetry (LDV). The propeller set, designed to operate in uniform flow, was tested in the DTRC 24-in. water tunnel. Axial, radial, and tangential induced velocity measurements were obtained forward of the two propellers, between the propeller set, and downstream of the aft propeller, with the propellers operating at the design condition.

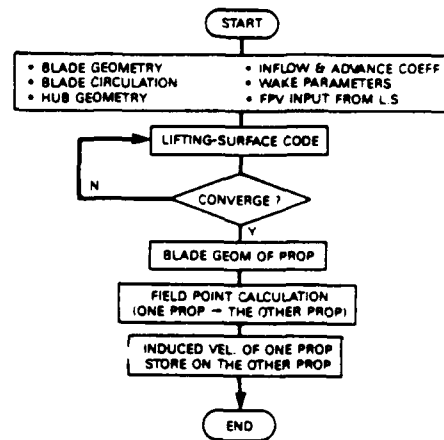


FIG. 5 FLOW CHART OF NEW CR LIFTING-SURFACE PROGRAM

The position of the trailing vortex wake geometry is traced by searching for the zero crossing point of the tangential velocity (i.e., $V_t=0$) versus radius. Despite the large number of data points which were collected, there are not enough data points to determine the complete slipstream. Data were obtained at two different locations downstream of the aft propeller. These include experiments 17 through 21. From the data collected in these experiments, one slipstream behind each propeller was derived. It has been plotted in Fig. 6. The contraction angles of the forward and aft propellers are 15° and 34° , respectively. It is believed that the contraction angle of the aft propeller is larger than that of the forward propeller because the induced velocity effect of the forward propeller on the aft propeller is more significant than the effect of the aft propeller on the forward propeller.

III. SAMPLE CALCULATION FOR A CR PROPELLER DESIGN

A CR propeller set, with a 7 blade forward propeller ($D = 16.5$ feet) and 5 blade aft propeller ($D = 15.826$ feet), has been designed for a surface ship. The propellers were designed for a speed of 20 knots with the rotational speeds for both propellers at 65 rpm. The traditional design procedure was used for this design. In this section, a comparison between the traditional design procedure (TDP) and the new design procedure (NDP) is given.

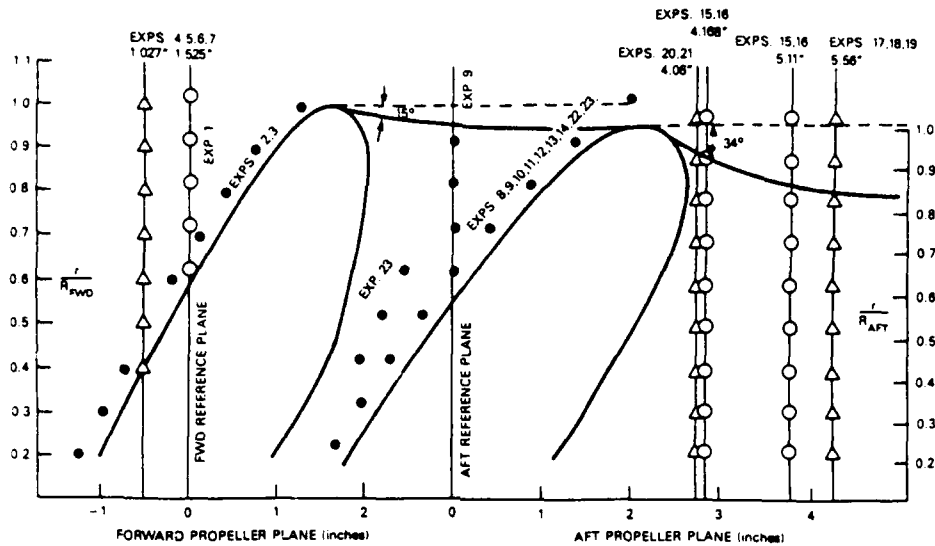


FIG. 6 SLIPSTREAM CONTRACTION OF A CR PROPELLER USING LDV MEASUREMENTS
(This figure is based on Nagle and McMahon (14))

For the forward propeller design, Fig. 7 shows the radial distribution of the axial velocity, $u_{aA,F}$, induced by the aft propeller at the forward propeller reference line. The magnitude of $u_{aA,F}$ from TDP (lifting-line model) is smaller than that from NDP (the lifting-surface model) because NDP includes the thickness, rake and skew effects. This indicates that the torque of NDP will be larger than that of TDP. However, the magnitude of $u_{aA,F}$ is very small because the wake induced by the aft propeller does not significantly affect the forward propeller.

The variation of the radial velocity, $u_{rA,F}$, induced by the aft propeller at the forward propeller reference line is shown in Fig. 8. The magnitude of the radial velocity from the TDP is equal to zero, while that of NDP is small and oriented outward. This indicates that the amount of wake contraction for the forward propeller will be reduced due to the effect of the aft propeller. Fig. 9 shows that the tangential velocity, $u_{tA,F}$, induced by the aft propeller at the forward propeller reference line is zero because the wake of the aft propeller can not affect the forward propeller.

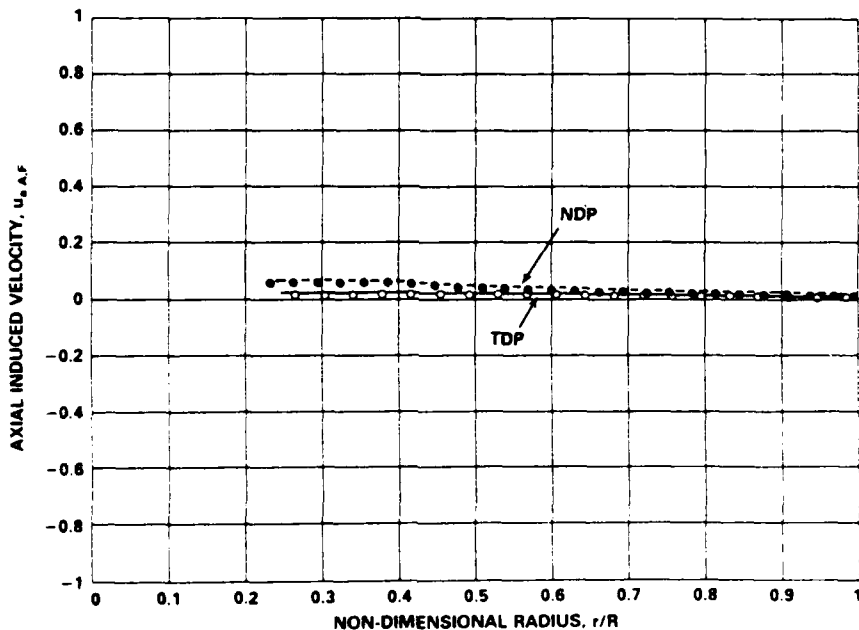


FIG. 7 COMPARISON OF RADIAL DISTRIBUTION OF AXIAL VELOCITY INDUCED BY AFT PROPELLER ON FORWARD PROPELLER

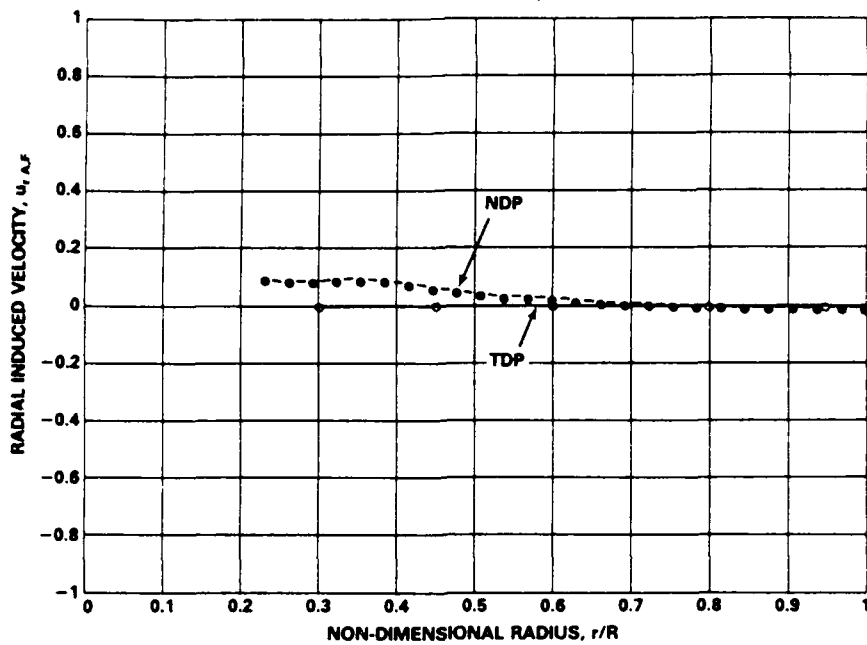


FIG. 8 COMPARISON OF RADIAL DISTRIBUTION OF RADIAL VELOCITY INDUCED BY AFT PROPELLER ON FORWARD PROPELLER

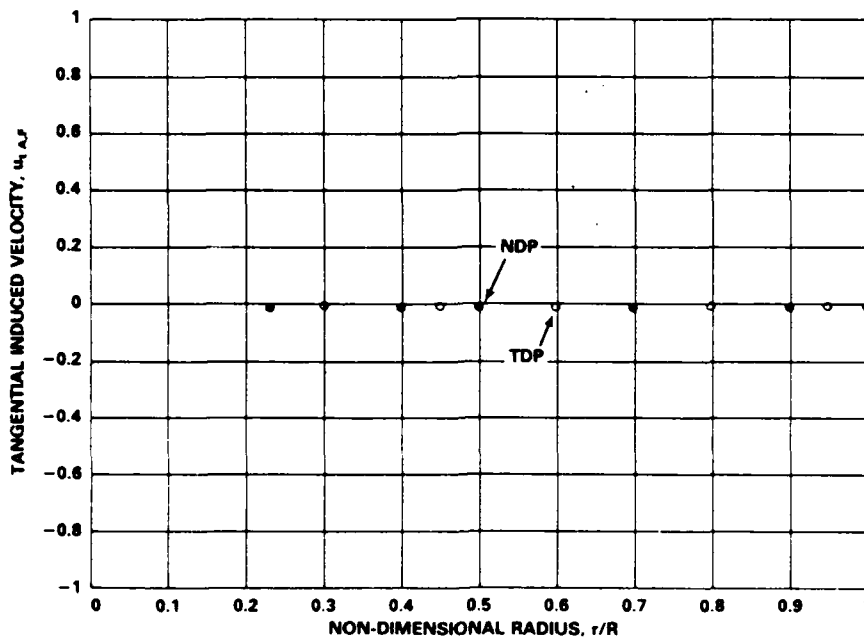


FIG. 9 COMPARISON OF RADIAL DISTRIBUTION OF TANGENTIAL VELOCITY INDUCED BY AFT PROPELLER ON FORWARD PROPELLER

Since the differences in the induced velocities predicted by TDP and NDP are very small for the forward propeller, the pitch and the camber distributions should be similar. The radial distribution of the pitch-diameter ratio, P/D, is affected by both the inflow, the propeller induced velocities, and by the rotational speed. Because of the identical rotational speeds and inflow, the induced velocities dominate the differences in the pitch-diameter ratio, shown in Fig. 10, between the propellers designed using TDP and NDP. The magnitude of P/D from NDP is larger than that from TDP because $u_{aA,F}$ from NDP is larger. To maintain the same thrust, the camber ratio, f_M/c , of NDP should be smaller than that of TDP except near the hub. This is because NDP includes hub image effects (see Fig. 11). The thrust coefficient, K_T , the torque coefficient, K_Q , and the open water efficiency, η_o , are given as a function of drag coefficient, C_D , in Fig. 12. η_o from NDP is smaller than that of TDP because the torque of NDP is larger than that of TDP.

As for the aft propeller design, Fig. 13 shows the axial velocity, $u_{aF,A}$, induced by the forward propeller at the aft propeller reference line. The magnitude of $u_{aF,A}$ from TDP is smaller than that from NDP near both the hub and the tip because NDP includes the thickness, rake and skew effects. Thus, it is expected that NDP should have higher torque than TDP. The magnitude of $u_{aF,A}$ is higher than $u_{aA,F}$ because the wake of the forward propeller affects the aft

propeller more than that of the aft propeller affects the forward propeller. As Fig. 14 shows, the radial velocity, $u_{rF,A}$, induced by the forward propeller at the aft propeller reference line has zero value for TDP because the lifting-line model does not account for the radial induced velocity. The NDP has an inward value which will increase the wake contraction of the aft propeller. The variation of the tangential velocity, $u_{tF,A}$, induced by the forward propeller at the aft propeller reference line is shown in Fig. 15. The magnitude of the tangential velocity from NDP is higher near the tip and lower near the hub.

The pitch-diameter ratios from the designs developed with TDP and NDP demonstrate differences near the hub but not the tip, as shown in Fig. 16. It is apparent that the higher pitch from NDP near the hub is caused by the higher $u_{aF,A}$ and the lower $u_{tF,A}$ from NDP than from TDP. On the contrary, the small differences in the pitch near the tip are due to increases in both $u_{aF,A}$ and $u_{tF,A}$ when computed by NDP. Fig. 17 shows the radial distribution of the camber, f_M/c . It can be seen that the magnitude of camber from NDP is lower than that from TDP, especially near the tip. The reverse camber near the tip may be caused by the sharp decrease of the chord distribution near that region. Fig. 18 shows K_T , K_Q , and η_o versus C_D . The value of η_o from NDP is smaller than that from TDP because the thrust from NDP increases but the torque increases even more.

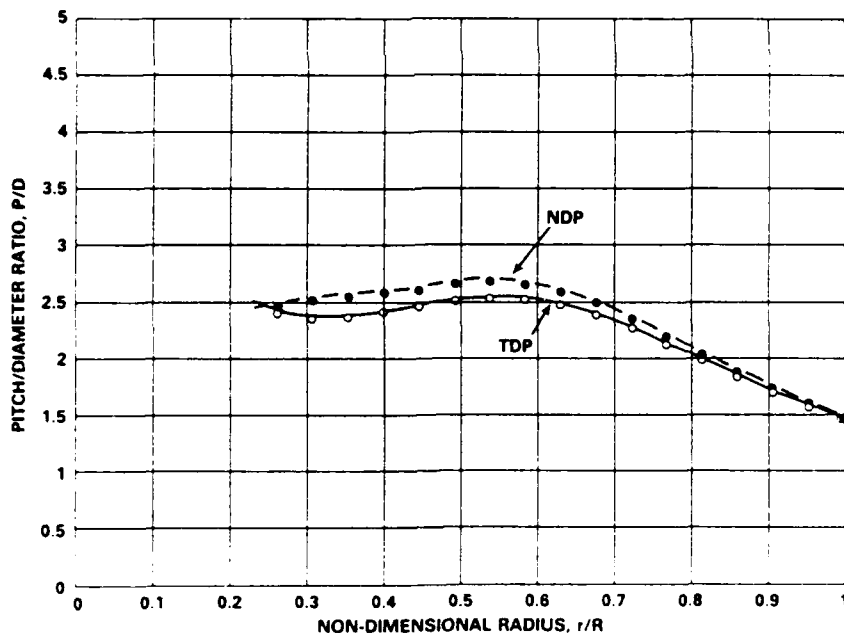


FIG. 10 COMPARISON OF RADIAL DISTRIBUTION OF PITCH/DIAMETER RATIO FOR FORWARD PROPELLER

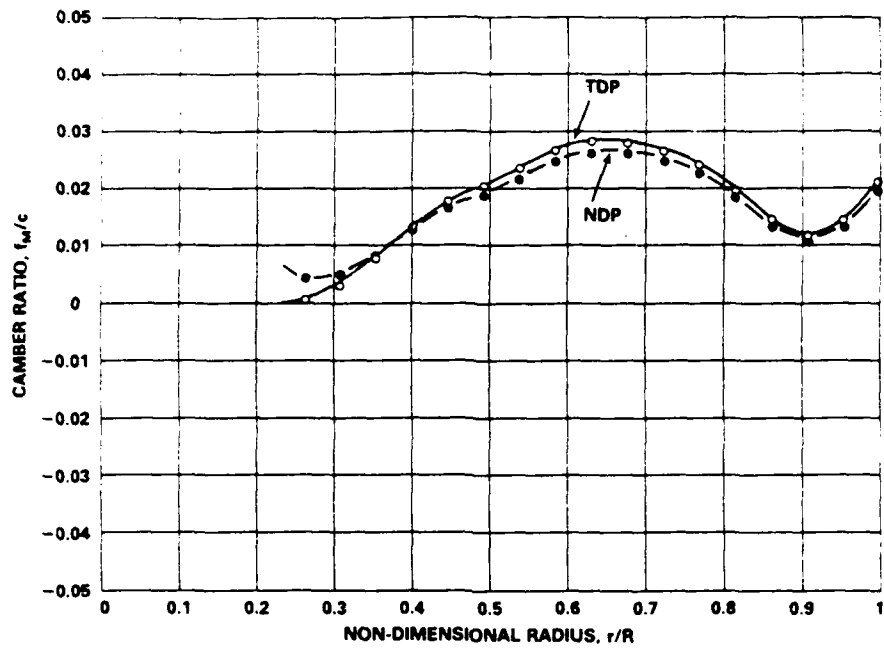


FIG. 11 COMPARISON OF RADIAL DISTRIBUTION OF CAMBER RATIO FOR FORWARD PROPELLER

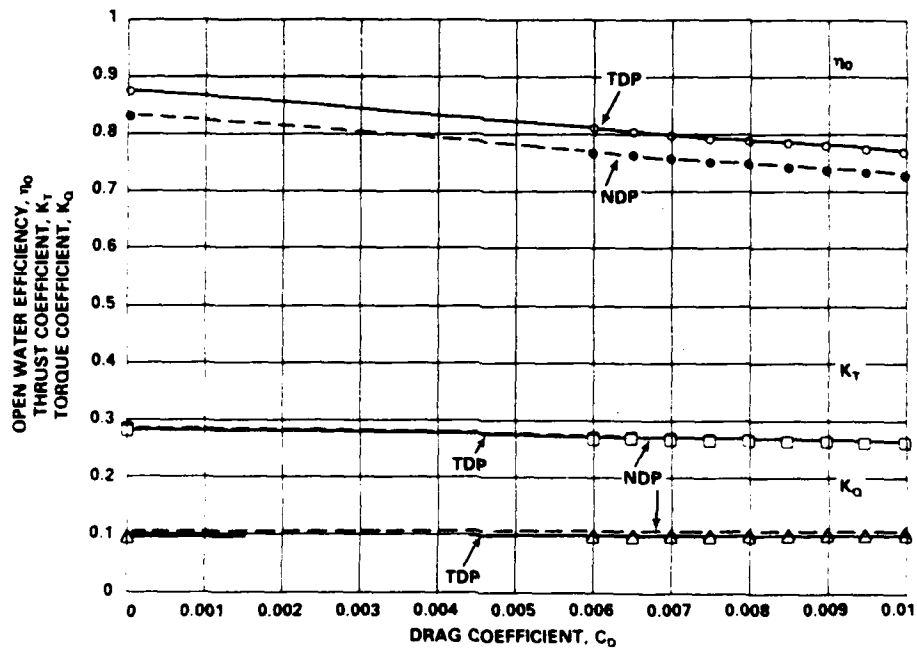


FIG. 12 COMPARISON OF OPEN WATER EFFICIENCY, THRUST COEFFICIENT, AND TORQUE COEFFICIENT VS. DRAG COEFFICIENT FOR FORWARD PROPELLER

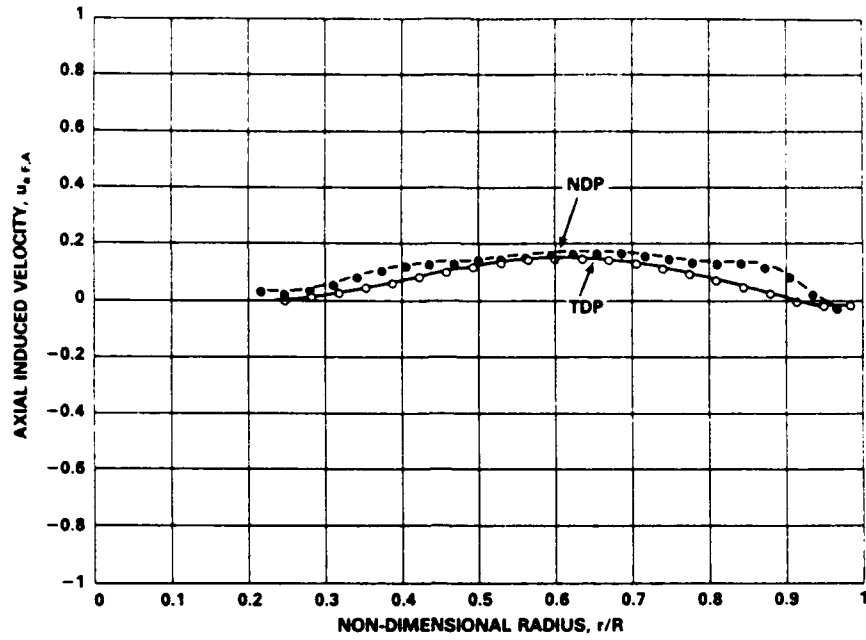


FIG. 13 COMPARISON OF RADIAL DISTRIBUTION OF AXIAL VELOCITY INDUCED BY FORWARD PROPELLER ON AFT PROPELLER

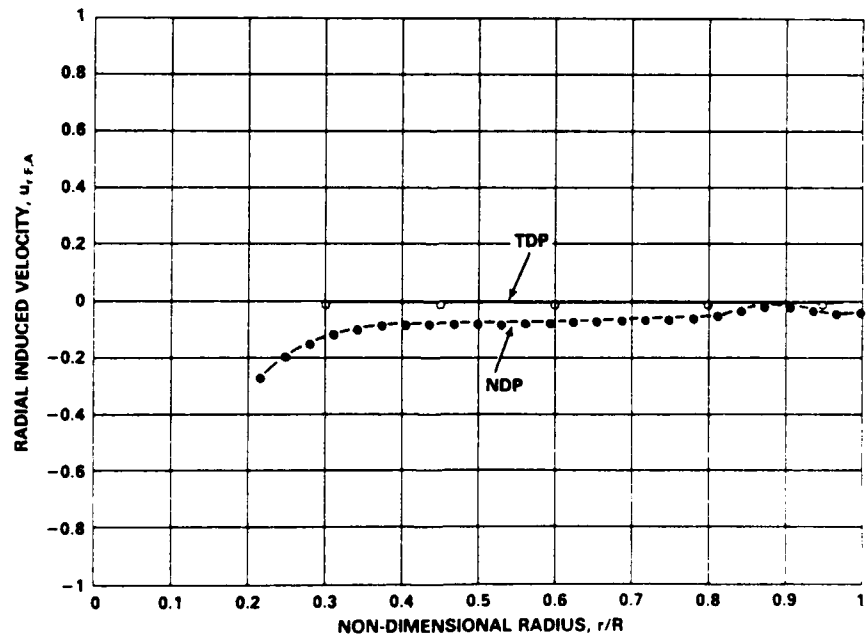


FIG. 14 COMPARISON OF RADIAL DISTRIBUTION OF RADIAL VELOCITY INDUCED BY FORWARD PROPELLER ON AFT PROPELLER

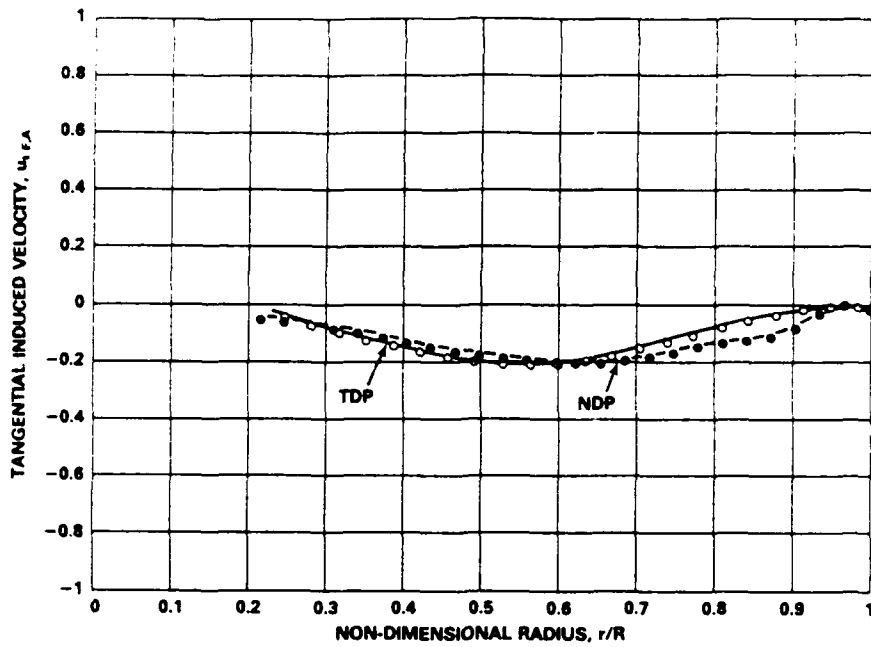


FIG. 15 COMPARISON OF RADIAL DISTRIBUTION OF TANGENTIAL VELOCITY INDUCED BY FORWARD PROPELLER ON AFT PROPELLER

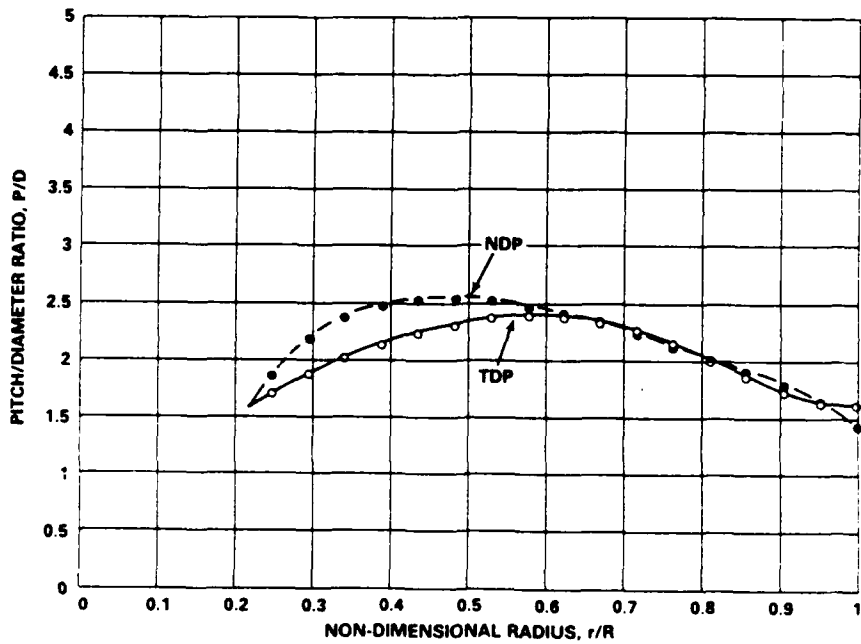


FIG. 16 COMPARISON OF RADIAL DISTRIBUTION OF PITCH/DIAMETER RATIO FOR AFT PROPELLER

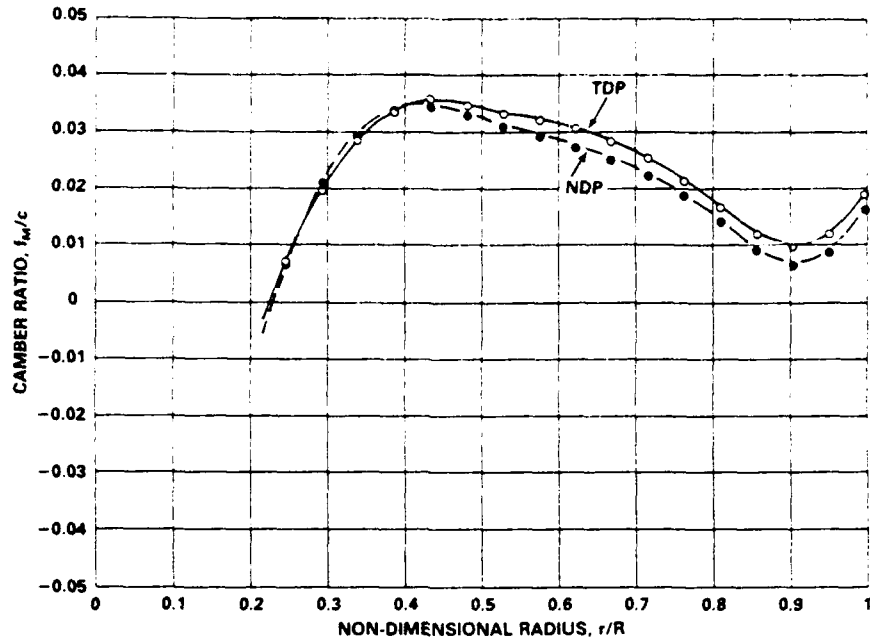


FIG. 17 COMPARISON OF RADIAL DISTRIBUTION OF CAMBER RATIO FOR AFT PROPELLER

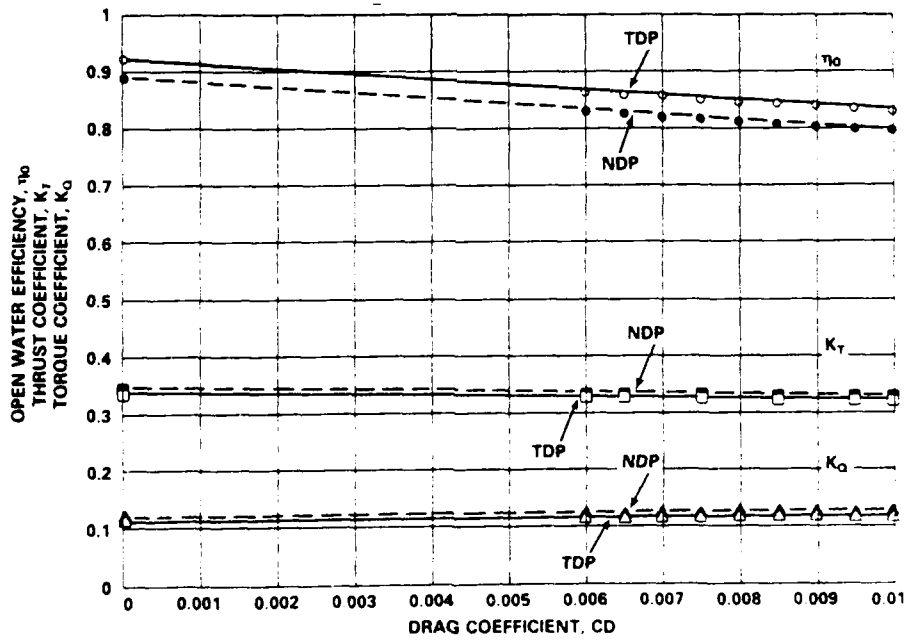


FIG. 18 COMPARISON OF OPEN WATER EFFICIENCY, THRUST COEFFICIENT, AND TORQUE COEFFICIENT VS. DRAG COEFFICIENT FOR AFT PROPELLER

IV. SUMMARY

A new lifting-surface computer program for the detailed design of the individual propellers of a CR set has been developed (see Chen and Reed (15)). In the traditional design procedure, the lifting-surface program computed the induced velocities from one propeller on the other from lifting-line calculations. The new design program computes the induced velocities from lifting-surface theory. Additionally, the hub portion of the program has been modified to take into account the velocities induced by one propeller on the hub of the other propeller. The shape and distribution of the wakes shed from the two propellers are adjusted based on LDV measurements of induced velocities. Nevertheless, the adjustment is very crude due to a limited amount of data.

A sample calculation which shows the comparison between the traditional and the new design procedures was shown. The results from the two design procedures look fairly consistent with each other except near the hub region. This consistency is because both procedures input the same circulation distribution. However, adding hub effects at the lifting-line step can produce a much different circulation distribution and the results should be quite different. The present study indicates that the use of interaction velocities calculated from the lifting-line model is sufficiently accurate for design use when the propeller loadings are moderate, and the propellers are not too close to each other.

V. CONCLUSIONS AND RECOMMENDATIONS

The conclusions from this study are as follows.

1. The new lifting-surface design procedure, which includes automatic induced velocity computation, hub effects, and empirical adjustment for wake contraction, is a better propeller design method than previously used.

2. The capability of this new lifting-surface program is not restricted to CR propellers but can be used to design other compound marine propulsors such as vane wheel propulsors.

There are several recommendations for further study of this topic.

1. The effects of propeller load distribution and spacing need to be further investigated to determine when the use of lifting-surface theory is mandated for predicting the mutual interaction velocities.

2. Detailed LDV measurements of the flow velocity in the vicinity of CR propellers need to be performed to get further information on the shape and distribution of the wakes shed from the two propellers.

3. An unsteady force calculation design method for CR propellers needs to be developed.

VI. ACKNOWLEDGMENTS

The authors would like to thank Mr. Carl Schott for providing the field point velocity program of the single screw propeller. Funding for this work was provided by Office of Naval Technology under ship and submarine technology program, program element 62543N.

VII. REFERENCES

1. "International Towing Tank Conference Standard Symbol 1976," The British Ship Research Association, BSRA Technical Memorandum No. 500 (May 1976).
2. Lerbs, H. W., "Contrarotating Optimum Propellers Operating in a Radially Non-Uniform Wake," David Taylor Model Basin Report 941 (May 1955).
3. Morgan, W. B., "The Design of Counterrotating Propellers Using Lerb's Theory," Trans. SNAME, Vol. 68 (1960) pp. 6-38.
4. Lerbs, H. W., "Moderately Loaded Propellers with a Finite Number of Blades and an Arbitrary Distribution of Circulation," Trans., SNAME, Vol. 60, (1952) pp. 73-117.
5. Eckhardt, M. K. and W. B. Morgan, "A Propeller Design Method," Trans., SNAME, Vol. 63 (1955) pp. 325-374.
6. Caster, E. B. and T. A. Lafone, "A Computer Program for the Preliminary Design of Contrarotating Propellers," DTNSRDC Ship Performance Department Report No. SPD-596-01 (Dec 1975).
7. Nelson, D. M., "Development and Application of a Lifting-Surface Design Method for Counterrotating Propellers," Naval Undersea Center, TP-326 (1972).
8. Cox, B. D., "Contrarotating Propeller Theory and Design Application," HRA Report 83-002 (1983).
9. Reed, A. M., "A Lifting-Line Computer Program for Contrarotating Propellers," DTNSRDC Ship Performance Department Report (under review).
10. Wang, M. H., "Hub Effects in Propeller Design and Analysis," Department of Ocean Engineering, MIT Report 85-14 (1985).
11. Kerwin, J. E., "Flow Field Computations for Non-Cavitating and Cavitating Propellers," 14th Symposium on Naval Hydrodynamics, Ann Arbor, Michigan (1982).
12. Greeley, D. S. and J. E. Kerwin, "Numerical Methods for Propeller Design and Analysis in Steady Flow," Annual Meeting of SNAME, New York (1982).
13. Kerwin, J. E. and C.S. Lee, "Prediction of Steady and Unsteady Marine Propeller Performance by Numerical Lifting-Surface Theory," Trans., SNAME, Vol. 86 (1978) pp. 218-253.
14. Nagle, T. J. and J. F. McMahon, "Flow Velocity Measurements in the Vicinity of a Set of Contrarotating Research Propeller (Propellers 4866 and 4867) Using Laser Doppler Velocimetry," Ship Performance Department Report, DTNSRDC/SPD-594-04 (1985).
15. Chen, B. Y.-H. and A. M. Reed, "A Lifting-Surface Program for Contrarotating Propellers," Ship Performance Department Report, DTNSRDC/SPD-1232-01 (1987).

INITIAL DISTRIBUTION

Copies

Copies

1 ARMY CHIEF OF RES & DEV
 1 AER&DL
 3 CHONR
 1 Lib
 1 Rood
 1 Code 21
 4 ONR BOSTON
 4 ONR CHICAGO
 4 ONR LONDON, ENGLAND
 1 NRL
 2 USNA
 1 Lib
 1 Johnson
 1 NAVPGSCOL Lib
 1 NROTC & NAVADMINU, MIT
 1 NADC
 4 NOSC
 1 1311 Lib
 1 6005
 1 13111 Lib
 1 Mautner
 1 NSWC
 31 NAVSEA
 5 SEA 05R
 1 SEA 55
 3 SEA 55N
 1 SEA 55W
 3 SEA 56D
 1 SEA 56X
 3 SEA 56X1
 1 SEA 56X2
 3 SEA 56X4
 1 SEA 56X5
 1 SEA 56XP
 1 PMS-383
 1 PMS-392

NAVSEA (Continued)
 1 PMS-396
 1 PMS-399
 1 PMS-400
 1 SEA Tech Rep
 Bath, England
 2 DET NORFOLK
 (Sec 6660)
 2 MMA
 1 Lib
 1 Maritime Res Cen
 12 DTIC
 2 HQS COGARD
 1 US COAST GUARD (G-ENE-4A)
 1 LC/SCI & Tech Div
 2 NASA STIF
 1 DIR RES
 1 NSF ENGR DIV/Lib
 1 DOT Lib
 2 U CAL BERKELEY/DEPT NAME
 1 NAME Lib
 1 Webster
 1 U MISSISSIPPI DEPT OF M.E.
 1 Fox
 3 CIT
 1 AERO Lib
 1 Acosta
 1 Wu
 4 U IOWA
 1 Lib
 1 IHR/Kennedy
 1 IHR/Stern
 1 IHR/Patel

INITIAL DISTRIBUTION (Continued)

Copies		Copies	
3	U MICHIGAN/DEPT NAME 1 NAME Lib 1 Parsons 1 Vorus	1	WHOI OCEAN ENGR DEPT
		1	WPI ALDEN HYDR LAB Lib
		1	ASME/RES COMM INFO
3	MIT 1 BARKER ENGR Lib 2 OCEAN ENGR/Kerwin	1	ASNE
		1	SNAME/Tech Lib
3	STATE U MARITIME COLL 1 ARL Lib 1 ENGR DEPT 1 INST MATH SCI	1	AERO JET-GENERAL/Beckwith
		1	ALLIS CHALMERS, YORK, PA
4	PENN STATE U ARL 1 Lib 1 Henderson 1 Gearhart 1 Thompson	1	AVCO LYCOMING
		1	BAKER MANUFACTURING
		1	BIRD-JOHNSON CO/Norton
1	BOEING ADV AMR SYS DIV	1	DOUGLAS AIRCRAFT/Lib
1	BB&N/Jackson	2	EXXON RES DIV 1 Lib 1 Fitzgerald
1	BREWER ENGR LAB		
1	CAMBRIDGE ACOUS/Junger	1	FRIEDE & GOLDMAN/Michel
1	CALSPAN, INC/Ritter	1	GENERAL DYNAMICS, EB/Boatwright
1	STANFORD U/Ashley	1	GIBBS & COX/Lib
1	STANFORD RES INST Lib	1	ROSENBLATT & SON/Lib
2	SIT DAVIDSON LAB 1 Lib 1 Savitski	1	GRUMMAN AEROSPACE/Carl
		1	TRACOR HYDRONAUTICS/Lib
1	TEXAS U ARL Lib	1	INGALLS SHIPBUILDING
1	UTAH STATE U/Jeppson	1	INST FOR DEFENSE ANAL
2	VPI/DEPT AERO & OCEAN ENGR 1 Schetz 1 Kaplan	1	ITEK VIDYA
		1	LIPS Duran/Kress
2	WEBB INST 1 Ward 1 Hadler	1	LITTLETON R & ENGR CORP/Reed
		1	LITTON INDUSTRIES

INITIAL DISTRIBUTION (Continued)

Copies		Copies	Code	Name	
		1	152	Lin	
1	LOCKHEED, SUNNYVALE/Waid				
		1	1521	Day	
2	MCDONNELL DOUGLAS, LONG BEACH	1	1521	Karafiath	
	1 Cebeci	1	1521	Hurwitz	
	1 Hess				
		1	1522	Remmers	
1	MARITECH, INC/Vassilopoulos	1	1522	Wilson	
2	HRA, INC	1	154	McCarthy	
	1 Cox				
	1 Scherer	1	154.1	Yim	
1	NIELSEN ENGR/Spangler	1	1542	Huang	
1	NKF ASSOCIATES/Noonan	1	1544	Reed	
		20	1544	Chen	
1	NAR SPACE/Ujihara				
		1	156	Cieslowski	
2	ATLANTIC APPLIED RESEARCH				
	1 Brown	1	172	Krenzke	
	1 Greeley				
		1	1720.6	Rockwell	
1	PROPULSION DYNAMICS, INC				
		1	19	Sevik	
1	SPERRY SYS MGMT Lib/Shapiro				
		1	1901	Strasberg	
1	TETRA TECH PASADENA/Furuya				
		1	1905	Blake	
1	UA HAMILTON STANDARD/Cornell				
		1	1906	Biancardi	
	CENTER DISTRIBUTION	1	1942	Mathews	
		1	1962	Kilcullen	
Copies	Code	Name			
1	0120		10	522.4	Reports Control
1	12		1	522.1	TIC (C)
1	112.1	Nakonechny	1	522.2	TIC (A)
1	15	W.R. Morgan			
1	1506	Walden			
1	1508	Boswell			